Supporting Information

Carbon Dots with High Quantum Yield used for Fe^{3+} Detection, Information Encryption and Anti-counterfeiting

Daohan Zhang[1] · Lei Liu[1,2*] · Chunyan Li[1]

1 College of Chemical and Pharmaceutical Engineering, Hebei University of Science and Technology, Shijiazhuang 050018, China.

2 Hebei Provincial Key Laboratory of Medicinal Molecular Chemistry - State Key Laboratory Breeding Base, Shijiazhuang 050018, China.

* Corresponding author. E-mail: liulei@hebust.edu.cn

Contents

1. Measuring fluorescence quantum yield and fluorescence lifetime

The measurement of fluorescence quantum yield was conducted using a standard method. Quinine sulfate was used as the reference substance for determining the fluorescence quantum yield. By adhering to the equation:

$$Y_u = Y_s \times \frac{F_u}{F_s} \times \frac{A_s}{A_u} \times (\frac{\varphi_u}{\varphi_s})^2 \times 100\% \quad (1)$$

Where in " Y_u " is the quantum yield of target product, " Y_s " is the quantum yield of known reference quinine sulfate (quantum yield in water is 0.53), " F_u " is the fluorescence integrated area of target product, " F_s " is the quinine sulfate reference product Fluorescence integral area, "A_u" is the absorbance of the target product, "A_s" is the absorbance of the reference product of quinine sulfate, "$\frac{\varphi_u}{\varphi_s}$" is the ratio of the refractive index of the solvent, and the solvent is water.

All tested fluorescence decay curves could be well fitted with double exponential functions. The average lifetime savg of B-CDs with and without Fe^{3+} was determined by the following equation:

$$\tau_{avg} = \frac{B_1\tau_1^2 + B_2\tau_2^2}{B_1\tau_1 + B_2\tau_2} \quad (2)$$

Where $B_1$and B_2 are the pre-exponential factors, τ_1 and τ_2 are the decay times.

2. Supplementary figures and table S1

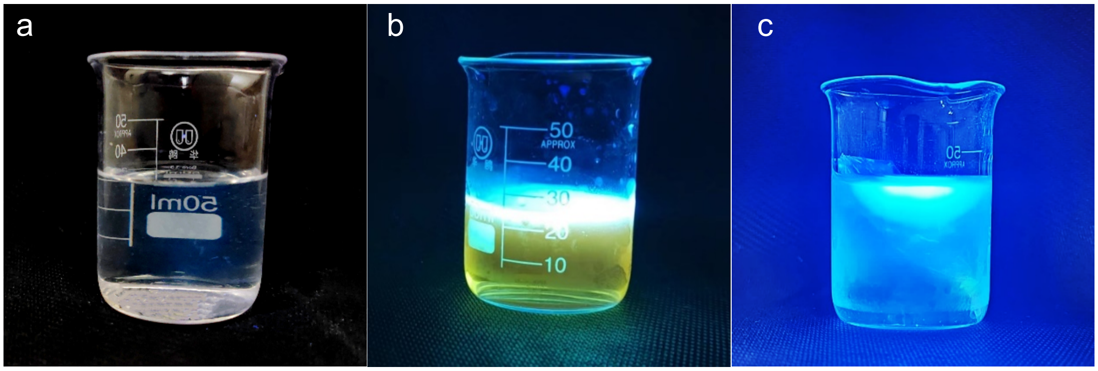

Figure S1 Fluorescence images of B-CDs: (a) Before microwave digestion; (b) After microwave digestion; (c) After dialysis.

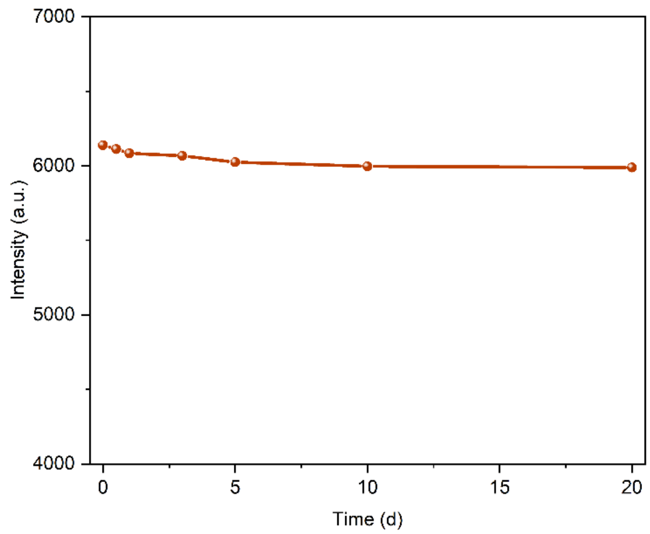

Figure S2 The change of fluorescence intensity of B-CDs over time (0-20d).

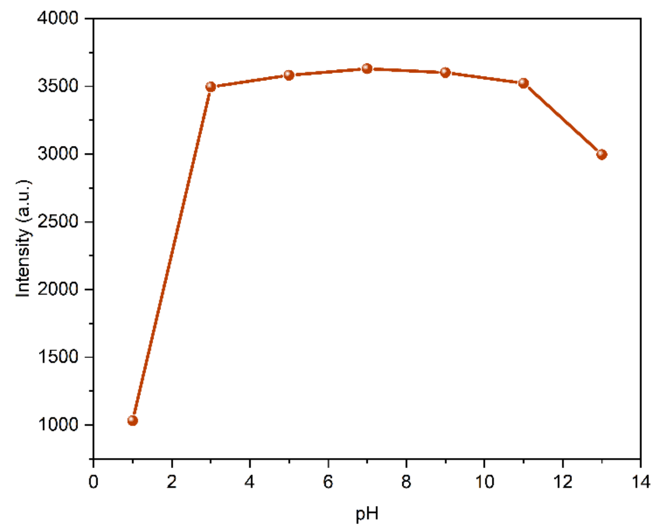

Figure S3 The fluorescence intensity of B-CDs varies with pH.

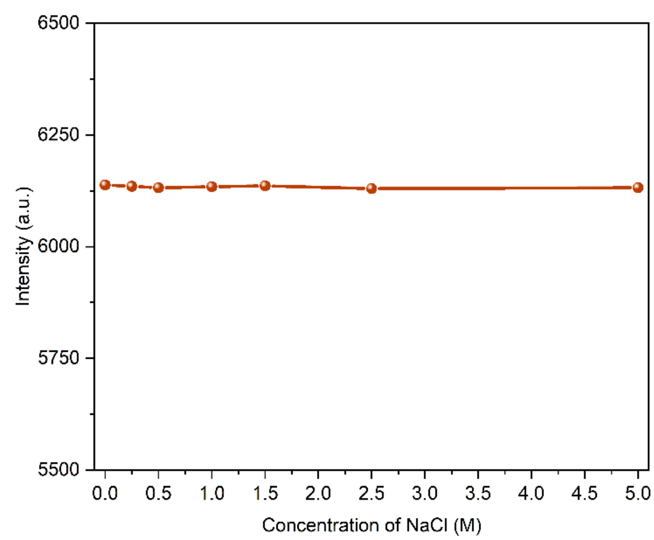

Figure S4 Effect of different ionic strengths (0-5.0M NaCl) on fluorescence intensity of B-CDs.

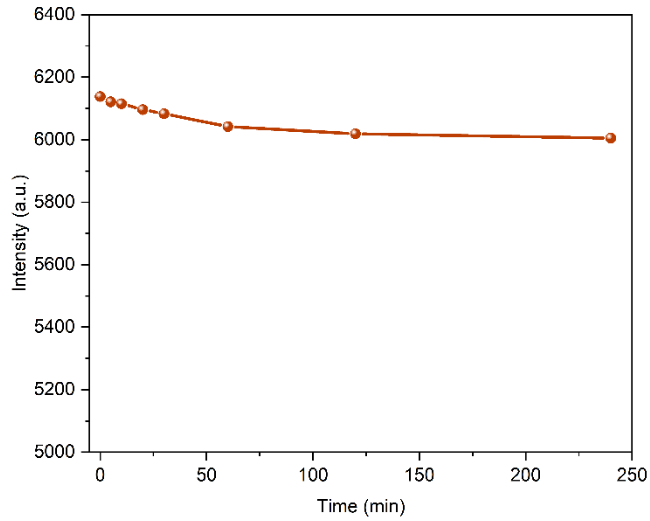

Figure S5 Fluorescence changes of B-CDs under 365nm UV irradiation (0-240min).

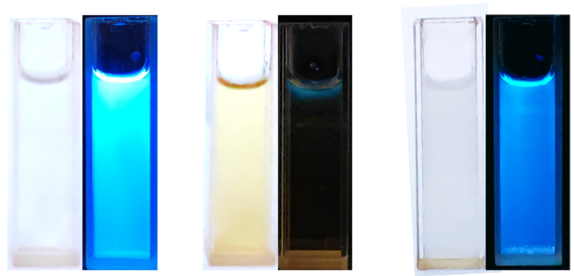

Figure S6 Fluorescence of the "on-off - on" model under daylight and 365n UV-light.

Table S1 Fe^{3+} detected by different substances

Category of test substance	Test substance/ material	Linear interval	LOD	Reference
CDs	Coffee grounds	0 - 2mM; R^2 = 0.996	2.25 µM	1
	Glu + PPD	0 - 100µM; R^2 = 0.995	1.2 µM	2
	(B-CQDs)/CdTe-Eu^{3+}	0.1 - 15µM; R^2 = 0.9956	53 nm	3
	Thiourea + OPD	0.3 - 70µM; R^2 = 0.9995	0.19 µM	4
	CA+OPD	**0.8 - 80µM; R^2=0.9931**	**0.095 µM**	**This article**
Metal-organic skeleton	$\{[Me_2NH_2][TbL]\cdot 2H_2O\}_n$	0 - 0.3mM; R^2 = 0.993	—	5
	JLU-MOF201-Y	—	2.21 µM	6
	JLU-MOF201-Tb		2.17 µM	
	GUPT-2	1 - 7µM; R^2 = 0.9967	0.446 µM	7
Metal nanocluster	INOS@ AuNCs	80-1000µM; R^2= 0.9995	5.4 µM	8
	GHRP-6-AuNCs	1.0 - 1100µM; R^2 = 0.996	14 µM	9
Organic small molecule	Rhodamine + amino acid derivatives	0 - 20µM; R^2 = 0.996	0.88 µM	10
	Spacer vinyl Rhodamine derivatives	1 - 50µM; R^2 = 0.996	102.3 nm	11
	Quinoline thiazole derivatives	0 - 100µM; R^2 = 0.996	3.12×10^{-4}M(QPT) 2.98×10^{-4}M(QBT)	12
Organic polymer	Eu complex copolymer microspheres	0 - 300µM; R^2 = 0.996	2.6 µM	13
	Tb complex copolymer microspheres	0 - 1500µM; R^2 = 0.996	2.1 µM	14

Table S2 Recovery rate of B-CDs to Fe^{3+} solutions with different concentrations

Concentration (μM)	Recovery rate (%)	RSD (%)
5	101.07	4.45
15	102.84	3.74
30	98.89	2.58
50	100.19	3.02
75	98.83	1.34

3. References

(1) Jeong, G.; Park, C.; Yi, D.; Yang, H. Green synthesis of carbon dots from spent coffee grounds via ball-milling: Application in fluorescent chemosensors. *J. Cleaner Prod.* **2023**, *392*, 136250.

(2) Zhang, X.; Li, Y.; Wang, Y.; Liu, X.; Jiang, F.; Liu, Y.; Jiang, P. Nitrogen and sulfur co-doped carbon dots with bright fluorescence for intracellular detection of iron ion and thiol. *J. Colloid Interface Sci*. **2022**, *611*, 255-264.

(3) Huang, M.; Tong, C. A dual-emission ratiometric fluorescence probe for highly selective and simultaneous detection of tetracycline and ferric ions in environmental water samples based on a boron-doped carbon quantum dot/CdTe–Eu^{3+} composite. *Environ. Sci.: Nano* **2022**, *9*, 1712-1723.

(4) Liu, Q.; Niu, X.; Xie, K.; Yan, Y.; Ren, B.; Liu, R.; Li, Y.; Li, L. Fluorescent carbon dots as nanosensors for monitoring and Imaging Fe^{3+} and $[HPO_4]^{2-}$ Ions. *ACS Appl. Nano Mater*. **2021**, *4*, 190-197

(5) Wang, J.; Yu, M.; Chen, L.; Li, Z.; Li, S.; Jiang, F.; Hong, M. Construction of a stable lanthanide metal-organic framework as a luminescent probe for rapid naked-eye recognition of Fe^{3+} and acetone. *Molecules* **2021**, *26*, 1695.

(6) Hu, Q.; Xu, T.; Gu, J.; Zhang, L.; Liu, Y. A series of isostructural lanthanide metal–organic frameworks: effective fluorescence sensing for Fe^{3+}, 2, 4-DNP and 4-NP. *CrystEngComm* **2022**, *24*, 2759-2766.

(7) Wang, S.; Zheng, X.; Zhang, S.; Li, G.; Xiao, Y. A study of GUPT-2, a water-stable zinc-based metal–organic framework as a highly selective and sensitive fluorescent sensor in the detection of Al^{3+} and Fe^{3+} ions[J]. *CrystEngComm* **2021**, *23*, 4059-4068.

(8) Halawa, M.; Wu, F.; Nsabimana, A.; Lou, B.; Xu, G. Inositol directed facile "green" synthesis of fluorescent gold nanoclusters as selective and sensitive detecting probes of ferric ions. *Sens. Actuators, B* **2018**, *257*, 980-987.

(9) Li, H.; Huang, H.; Feng, J.; Luo, X.; Fang, K.; Wang, Z. Ai-Jun Wang,. A polypeptide-mediated synthesis of green fluorescent gold nanoclusters for Fe^{3+} sensing and bioimaging. *J. Colloid Interface Sci.* **2017**, *506*, 386-392.

(10) Li, H.; Liu, Z.; Jia, R. "Turn-on" fluorescent probes based on Rhodamine B/amino acid derivatives for detection of Fe^{3+} in water. *Spectrochim. Acta, Part A* **2021**, *247*, 119095.

(11) Shellaiah, M.; Thirumalaivasan, N.; Aazaad, B.; Awasthi, K.; Sun, K.; Wu, S.; Lin, M. Novel rhodamine probe for colorimetric and fluorescent detection of Fe^{3+} ions in aqueous media with cellular imaging. *Spectrochim. Acta, Part A* **2020**, *242*,118757.

(12) Shyamsivappan, S.; Saravanan, A.; Vandana, N.; Suresh, T.; Suresh, S.; Nandhakumar, R.; Mohanet, P.S. Novel quinoline-based thiazole derivatives for selective detection of Fe^{3+}, Fe^{2+}, and Cu^{2+} ions. *ACS omega* **2020**, *5*, 27245-27253.

(13) Zhang, C.; Luo, J.; Li W.; Ou, L.; Yu, G.; Pan, C. Preparation and sensing properties of covalent-linked europium complex monodisperse polystyrene microspheres†. *Chem. J. Chinese Universities*, **2019**, *40*, 153.

(14) Zhang, C. Y., Luo, J. X., Li, W. J., Ou, L. J., Yu, G. P., Pan, C. Y. Selective recognition of Fe (III) in aqueous environment over covalently‐bonded Tb‐complex‐containing fluorescent porous copolymer microspheres. *Macromol. Chem. Phys.* **2018**, *219*, 1800403.